High Q^2 Behavior of the Proton Structure Function through the Balitsky–Kovchegov Equation

Wei Kou[1,2], Gang Xie[1,3], Xiaopeng Wang[1,2,4], Chengdong Han[1,2*], and Xurong Chen[1,3,5*]

[1]*Institute of Modern Physics, Chinese Academy of Sciences, Lanzhou 730000, China*
[2]*School of Nuclear Science and Technology, University of Chinese Academy of Sciences, Beijing 100049, China*
[3]*University of Chinese Academy of Sciences, Beijing 100049, China*
[4]*Lanzhou University, Lanzhou 730000, China*
[5]*Southern Center for Nuclear Science Theory, Institute of Modern Physics, Chinese Academy of Sciences, Huizhou 516000, China*

(Received 3 December 2024; accepted manuscript online 12 February 2025)

Numerous experimental and theoretical investigations have highlighted the power law behavior of the proton structure function $F_2(x, Q^2)$, particularly the dependence of its power constant on various kinematic variables. In this study, we analyze the proton structure function F_2 employing the analytical solution of the Balitsky–Kovchegov equation, with a focus on the high Q^2 regime and small x domains. Our results indicate that as Q^2 increases, the slope parameter λ, which characterizes the growth rate of F_2, exhibits a gradual decrease, approaching a limiting value of $\lambda \approx 0.41 \pm 0.01$ for large Q^2. We suggest that this behavior of λ may be attributed to mechanisms such as gluon overlap and the suppression of phase space growth. To substantiate these conclusions, further high-precision electron–ion collision experiments are required, encompassing a broad range of Q^2 and x.

DOI: 10.1088/0256-307X/42/3/031201 CSTR: 32039.14.0256-307X.42.3.031201

1. Introduction. Over the last two decades, the leading order (LO) and next-to-leading order (NLO) formulations of the Balitsky–Fadin–Kuraev–Lipatov (BFKL) equation[1–3] have been examined by L. N. Lipatov *et al.*[4–11] using the Green's function approach. They contended that the BFKL equation should be regarded as an eigen-equation with an eigenvalue ω_n. The authors in Ref. [4] argued that the discrete, asymptotically free BFKL Pomeron was initially shown to describe HERA data at low x and high Q^2. Most of the deep inelastic scattering (DIS) data provided by HERA are well described by the Dokshitzer–Gribov–Lipatov–Altarelli–Parisi (DGLAP) equations,[12–15] which are presented through the lens of renormalization group evolution.[16] Nonetheless, the discussion surrounding HERA data in the small x region has initiated the combination of the DGLAP and BFKL equations. It should be noted that the variation of the scattering cross-section with energy must satisfy the unitarity limit naturally; conversely, the BFKL equation, as a linear evolution equation, could challenge this property in the high-energy region. Fortunately, the infinite growth of gluons appears to be suppressed by certain processes. The saturation behavior of gluons is discussed in Refs. [17–19] (and references cited therein). The Balitsky–Kovchegov (BK) equation[20–23] represents a nonlinear evolution of gluons and serves as a mean-field approximation of the Jalilian–Marian–Iancu–McLerran–Weigert–Leonidov–Kovner (JIMWLK) equation.[24–27] The BK equation effectively describes gluon behavior in the small x region. In a previous work, some of us obtained an analytical solution of the BK equation in momentum space through a novel approach.[28]

The HERA collaboration provides high-precision data for the proton structure function F_2, making it a key resource for studying the behavior of F_2 under small x and large Q^2 conditions. The behavior of the structure function in the small x region is generally understood by analyzing its slope parameter λ,[29] defined as $\lambda \propto \partial \ln F_2 / \partial \ln(1/x)$. A significant body of previous work comprehensively addresses this topic[4–11,30–36] (and references cited therein). In recent years, physicists have offered various explanations for and fitting results related to the new HERA data.[37,38] Compared to the range of Q^2 explored in the data, several theoretical studies have provided results for the parameter λ as a function of Q^2 only in the intermediate region, such as $\mathcal{O}(200\,\mathrm{MeV}^2)$.[32,35,39,40] It is important to note that the structure function F_2 data at very high Q^2 pertain predominantly to the large x scale. These considerations lead us to explore the double-asymptotic-scaling (DAS) phenomenon, which describes the limits as $Q^2 \to \infty$ and $x \to 0$.

In the present work, we combine experimental findings and QCD evolution theory to analyze the proton structure function from the perspective of the BK equation. Based on the analytical solution presented in previous work,[28] we calculate the proton structure function F_2 at higher Q^2 and analyze the small x behavior by fitting the computed results. The organization of this paper is as follows. In

*Corresponding author. Email: chdhan@impcas.ac.cn; xchen@impcas.ac.cn
© 2025 Chinese Physical Society and IOP Publishing Ltd. All rights, including for text and data mining, AI training, and similar technologies, are reserved.

Section 2, we briefly introduce the methods and principles for calculating the proton structure function F_2 using the analytical solution of the BK equation from Ref. [28]. In Section 3, we discuss how to obtain the structure function F_2 and its corresponding effective slope parameter λ at high energies. In Section 4, we highlight the interesting results from Section 3. Finally, the conclusions of this work are presented in Section 5.

2. Formalism. We consider the high-energy scattering process using the dipole model (see Fig. 1). The high-speed moving photon fluctuates a $q\bar{q}$ pair from the QCD vacuum, forming a dipole. The total cross section for the overall $\gamma^* p$ scattering is represented by integrating the dipole cross section with the photon wave functions.[41–43] The momentum space formulation of the dipole scattering cross section can be obtained through Fourier transform. If the transverse profile of the proton is considered as an isotropic disk with radius R_p, the dipole scattering cross section is proportional to the forward scattering amplitude $\mathcal{N}(r, Y)$, which depends on the dipole transverse size r and rapidity Y as described in Ref. [44]:

$$\sigma_{\mathrm{dip}}^{\gamma^* p}(r, Y) = 2\pi R_\mathrm{p}^2 \mathcal{N}(r, Y), \tag{1}$$

where R_p is taken to be the electromagnetic radius of the proton.

Based on the above information, the structure function of proton can be expressed in momentum space as[44,45]

$$\begin{aligned} &F_2(x, Q^2) \\ &= \frac{Q^2 R_\mathrm{p}^2 N_\mathrm{c}}{4\pi^2} \int_0^\infty \frac{\mathrm{d}k}{k} \int_0^1 \mathrm{d}z |\tilde{\Psi}(k^2, z; Q^2)|^2 \mathcal{N}(k, Y), \end{aligned} \tag{2}$$

with the Fourier transform

$$\begin{aligned} \mathcal{N}(k, Y) &= \frac{1}{2\pi} \int \frac{\mathrm{d}^2 r}{r^2} \mathrm{e}^{\mathrm{i}\boldsymbol{k}\cdot\boldsymbol{r}} \mathcal{N}(r, Y) \\ &= \int_0^\infty \frac{\mathrm{d}r}{r} J_0(kr) \mathcal{N}(r, Y). \end{aligned} \tag{3}$$

The photon wave functions $\tilde{\Psi}$ in Eq. (2) can be found in Ref. [44] in momentum space. It is important to note that not only DIS calculations but also the vector meson diffractive production process has a similar wave function representation for calculations.[43,46]

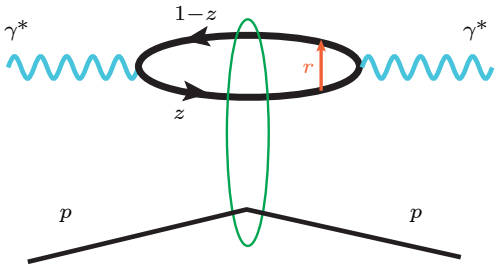

Fig. 1. The elastic scattering of a virtual photon on a proton in the dipole representation.[43]

We will now handle the forward scattering amplitude using the method described in Ref. [28]. The BK equation is rewritten as the Fisher-KPP equation[47] with appropriate variable substitutions. More specifically, the BK equation in momentum space can be described as a nonlinear variant of the BFKL equation,[19]

$$\begin{aligned} \frac{\partial \mathcal{N}(k, Y)}{\partial Y} &= \frac{\alpha_\mathrm{s} N_\mathrm{c}}{\pi} \chi\Big(-\frac{\partial}{\partial \ln k^2}\Big) \mathcal{N}(k, Y) \\ &\quad - \frac{\alpha_\mathrm{s} N_\mathrm{c}}{\pi} \mathcal{N}^2(k, Y), \end{aligned} \tag{4}$$

where $\chi(\lambda) = \psi(1) - \frac{1}{2}\psi(1-\frac{\lambda}{2}) - \frac{1}{2}\psi(\frac{\lambda}{2})$ is the BFKL kernel with the digamma function $\psi(\lambda) = \Gamma'(\lambda)/\Gamma(\lambda)$. In addition, the α_s is the strong coupling. In this work, we choose $Y = \bar{\alpha_\mathrm{s}} \log(1/x)$ with $\bar{\alpha_\mathrm{s}} = \alpha_\mathrm{s} N_\mathrm{c}/\pi$.

We utilize the analytical solution of the BK equation obtained through the Homogeneous Balance method in Refs. [48–52], which can be expressed as[28]

$$\mathcal{N}(L, Y) = \frac{A_0 \mathrm{e}^{5A_0 Y/3}}{\Big[\mathrm{e}^{5A_0 Y/6} + \mathrm{e}^{[-\theta + \sqrt{A_0/6A_2}(L - A_1 Y)]}\Big]^2}. \tag{5}$$

Here, the variable $L = \ln(k^2/k_0^2)$ with the cutoff $k_0 = \Lambda_\mathrm{QCD} = 0.0\,\mathrm{MeV}$. The parameter values θ, A_0, A_1, and A_2 are referenced in Refs. [28,53] and can be obtained by fitting experimental data.

3. Structure Function $F_2(x, Q^2)$ in High Energies. In Ref. [44], the authors discussed in detail the process of calculating the structure function F_2, including the selection of parameters contained in the momentum space photon wave function. We employ the same formalism from Ref. [44] to derive several parameters in the analytical solution of the BK equation by fitting HERA data.[37,54] Considering the small x limit, we chose to fit the experimental data in the range $2.5\,\mathrm{GeV}^2 < Q^2 < 250\,\mathrm{GeV}^2$ because the quantity of data and the precision in this region are suitable.

According to the discussions in Ref. [28], we fixed the strong coupling constant $\bar{\alpha_\mathrm{s}} = 0.191$, which is effective in the energy range we considered. We need to emphasize that the strong coupling constant $\bar{\alpha_\mathrm{s}}$ is fixed because the primary focus of this work is on the behavior of the structure function at higher Q^2, where the coupling constant can be considered to have a negligible impact on the results. This simplification is well justified. The chosen value for the coupling constant has also been used to calculate the diffractive production processes of vector mesons,[55] successfully describing experimental data.[56–60] To calculate F_2 using Eq. (2), the color number N_c is set to 3, and the considerations regarding quark mass and flavor remain unchanged from those we used in Ref. [44]. Specifically, we set $m_u = m_d = m_q = 140\,\mathrm{MeV}$ and $m_\mathrm{c} = 1.4\,\mathrm{GeV}$ for the quark masses,[44] while the proton size is treated as the electromagnetic radius $R_\mathrm{p} = 4.23\,\mathrm{GeV}^{-1}$. For the selection of quark mass parameters in the photon wave function, we referred to the work of the GBW model.[42,61,62] In principle, the choice of these parameters can influence the results; however, we treat the photon wave function as a priori and base our discussion of the applicability of the BK equation's analytical solution on this assumption. Based on these fixed parameter selections, we utilize the HERA data to fit and obtain the parameters in Eq. (5). The fitting results are displayed in Fig. 2 (with partial fitting results), and the fitting parameters of Eq. (5) are determined as $A_0 = 0.5262 \pm 0.0024$, $A_1 = 1.4383 \pm 0.0133$, $A_2 = 0.1047 \pm 0.0008$, and $\theta = -0.4572 \pm 0.0110$.

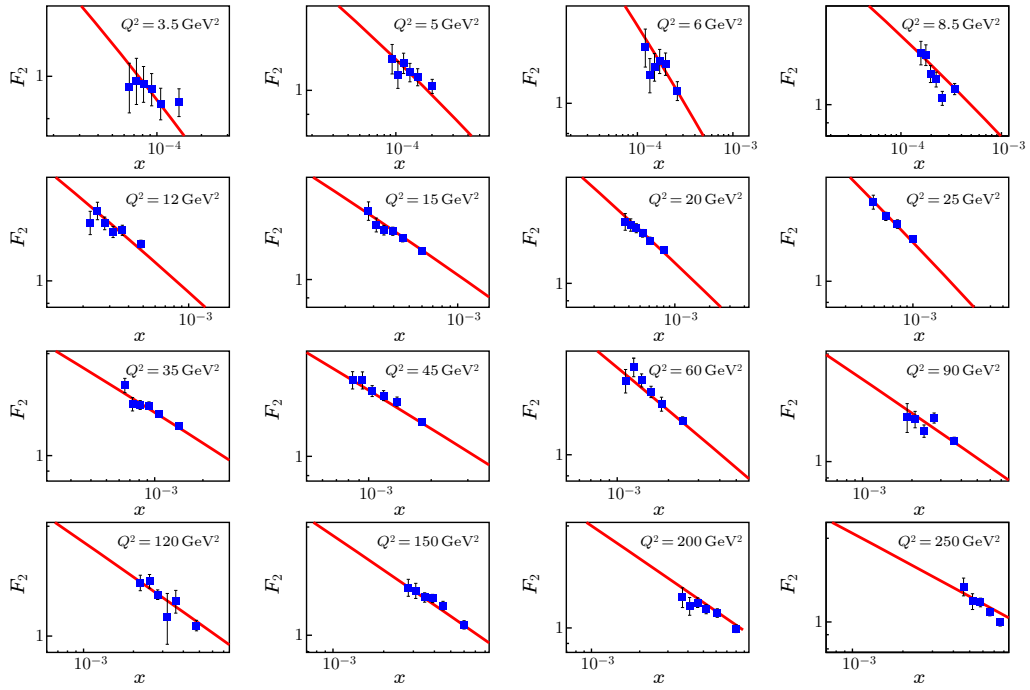

Fig. 2. x dependence of structure function $F_2(x, Q^2)$ with bins of Q^2. The data from H1 [54] (blue squares) are compared with our fit by analytical solution of BK [28] (red lines). The parameters determination is discussed in text.

Due to various experimental constraints, researchers are often particularly interested in the physics at the energy limits, such as $x \to 0$ and $Q^2 \to \infty$. Although this research may appear more mathematical in nature, it frequently yields intriguing predictions. In this study, we aim to investigate the small-x behavior of F_2 at higher Q^2. The slope parameter λ can be expressed as $\lambda \propto \partial \ln F_2 / \partial \ln(1/x)$ at different Q^2 values, as discussed in Ref. [30]. In the small-x range ($x < 0.01$), the structure function of the proton F_2 can be parameterized in a power-like form:

$$F_2(x, Q^2) = C x^{-\lambda(Q^2)}. \tag{6}$$

According to our calculations, the slope parameter λ is determined from the computed $F_2(x, Q^2)$ values using the BK equation and the dipole amplitude, in accordance with Eqs. (2) and (5). This will be discussed in the next section.

4. Results and Discussions. The BK equation, as a QCD theory, possesses predictive power under limiting conditions. Previous studies have generated theoretical predictions based on experimental data and appropriate assumptions, which have proven to be both effective and inspiring. In this work, we take this a step further by extending both the Bjorken scale x and Q^2 to their limits, utilizing the analytical solution of the BK equation. As we have discussed, we aim to characterize the behavior of F_2 under very high Q^2 conditions. We can readily extend F_2 to $Q^2 \sim \mathcal{O}(2000)\,\mathrm{GeV}^2$ through numerical calculations within the range $2.0 \times 10^{-5} < x < 1.0 \times 10^{-2}$. Utilizing the analytical solution (5) with the fitted parameters, the behavior of the slope factor λ is illustrated in Fig. 3.

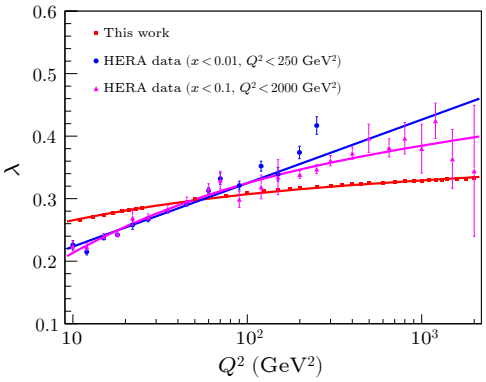

Fig. 3. Slope parameter λ v.s. energy scale Q^2. The red squares with error bars represent our calculations, determined by Eqs. (2), (5) and (6). The blue circles denote the extracted λ from Refs. [37,38] ($x < 0.01$, $Q^2 < 250\,\mathrm{GeV}^2$) and magenta triangles are extracted from same data from HERA [37] ($x < 0.1$, $Q^2 < 2000\,\mathrm{GeV}^2$). Red line represents the fitting result comes from Eq. (7) which describe the red points. The blue and magenta lines are fitting results of the corresponding color points, respectively.

Figure 3 presents the λ values extracted from the HERA data (blue and magenta points) [37,54] alongside our calculated results using the BK equation (red solid squares). We also provide parameterized formulas to describe the $\lambda - Q^2$ relation, expressed as

$$\lambda(Q^2) = a\Big(1 - \frac{b}{\ln(Q^2/\Lambda^2_{\mathrm{QCD}})}\Big) + c, \tag{7}$$

for the red and magenta points in Fig. 3, and

$$\lambda(Q^2) = A \ln\Big(\frac{Q^2}{\Lambda^2_{\mathrm{QCD}}}\Big) + B, \tag{8}$$

Table 1. Parameters determination according to Eqs. (7) and (8), using our calculations and HERA data. The results of the last two lines come from Refs. [37,38].

Parameters	$\Lambda_{\rm QCD}$ (MeV)	a	b	c	A	B
This work	200	0.162 ± 0.006	4.800 ± 0.168	0.244 ± 0.006		
Fits from Ref. [38]	200				0.044 ± 0.001	-0.020 ± 0.004
Fits from Ref. [37]	200	0.195 ± 0.017	10.657 ± 0.838	0.395 ± 0.016		

Table 2. The results for the λ constant obtained from the fits of the function (6) from Ref. [38] ($x < 0.01$), $Q^2 < 250\,\text{GeV}^2$.

Q^2 (GeV^2)	λ	$\delta\lambda$
0.35	0.110	0.008
0.4	0.082	0.009
0.5	0.100	0.009
0.65	0.121	0.011
0.85	0.150	0.014
1.2	0.133	0.013
1.5	0.142	0.009
2	0.159	0.007
2.7	0.169	0.005
3.5	0.173	0.004
4.5	0.189	0.004
6.5	0.200	0.003
8.5	0.208	0.004
10	0.226	0.007
12	0.215	0.005
15	0.237	0.003
18	0.242	0.003
22	0.258	0.007
27	0.267	0.004
35	0.280	0.003
45	0.292	0.004
60	0.313	0.005
70	0.332	0.009
90	0.321	0.007
120	0.352	0.008
150	0.339	0.011
200	0.373	0.010
250	0.417	0.014

Table 3. The results for the λ constant obtained from the fits of the function (6) from Ref. [37] ($x < 0.1$, $Q^2 < 2000\,\text{GeV}^2$).

Q^2 (GeV^2)	λ	$\delta\lambda$
10	0.224	0.008
12	0.223	0.006
15	0.240	0.004
18	0.244	0.005
22	0.269	0.012
27	0.271	0.005
35	0.284	0.006
45	0.296	0.007
60	0.316	0.008
70	0.330	0.014
90	0.299	0.013
120	0.319	0.019
150	0.334	0.0281
200	0.339	0.006
250	0.347	0.007
300	0.361	0.008
400	0.373	0.010
500	0.396	0.023
650	0.381	0.014
800	0.397	0.025
1000	0.380	0.039
1200	0.425	0.028
1500	0.364	0.047
2000	0.345	0.105

for the blue points.[38] In these equations, the QCD cutoff $\Lambda_{\rm QCD} = 200\,\text{MeV}$ is fixed. We use Eq. (7) to fit our calculations and the HERA data[37] (magenta triangles, $Q^2 < 2000\,\text{GeV}^2$). All parameter information is provided in Table 1, Table 2, and Table 3, respectively.

Let us consider this formula. In contrast to the logarithmic growth of λ with Q^2 discussed in other works,[39,40] we find that the rate of increase of λ decreases slowly with increasing Q^2, as indicated by $\mathrm{d}\lambda/\mathrm{d}Q^2|_{Q^2\to\infty} = 0$. This behavior resembles that of the running strong coupling constant in the extreme high-energy limit (see Ref. [63] and references cited therein). From Eq. (7), we consider the scenario where Q^2 approaches infinity. At this point, λ shows minimal growth with respect to Q^2, and its value reaches $\lambda(Q^2 \to \infty) = a + c \simeq 0.41 \pm 0.01$. This value may represent the upper limit that λ will attain. The "frozen" λ signifies that there is no change even if Q^2 continues to rise, leading to fixed rates of variation for the x-dependence of F_2. We also examined the selection of the fitting range for F_2 data and found no significant differences in the parameters C and λ [as defined in Eq. (6)] between $x < 0.01$ and $x < 0.001$ under these conditions.

To explain the "frozen" λ, we investigate the behavior of gluons in high-energy $\gamma^* p$ scattering using the BK equation. The parameter λ serves as a power index that represents the rate of gluon emissions per unit of rapidity from a high-speed dipole.[29,38] The formation of the structure function is expressed as[4,5]

$$F_2(x,\, Q^2) = \int_x^1 \mathrm{d}z \int \frac{\mathrm{d}k}{k} \Phi_{\rm DIS}(z,\, Q,\, k)\, xg\Big(\frac{x}{z},\, k\Big), \quad (9)$$

where $xg(\frac{x}{z},\, k)$ denotes the unintegrated gluon density defined in Ref. [4], expressed in the form of a power law with index λ (or the eigenvalue of the BFKL equation ω_n). On one hand, the invariant λ in the high Q^2 region indicates that the gluon emission rate has reached equilibrium. The behavior of λ we obtained aligns well with discussions and results from previous works.[61,64,65] On the other hand, as Q^2 increases and x decreases,[38] the phase space for gluon emissions expands rapidly. When the number of gluons becomes large, they begin to overlap, which limits the growth of phase space and ultimately results in a particular value, consistent with the requirements of unitarity in QCD theory.

Our results are built upon previous related works,[4–11,30–36] which generalize the Q^2-dependence of λ to higher Q^2 situations. However, in this work, we

have made certain approximations, such as the selection of fixed strong coupling constants. This approximation implies that we consider the calculation results to be more significant at specific Q^2 values, while at very low or high Q^2, discrepancies may arise (see Fig. 3). We argue that it is feasible to use the BK equation to investigate the proton structure function, despite these approximations. Our results are grounded in QCD evolution theory, and the BK equation has been proven to be a valuable tool in the study of DIS and diffraction processes.[17–19] The challenges we encountered are expected to be addressed in future research, particularly through the application of the BK equation with running coupling constants[55,66] or the numerical solution of the JIMWLK equation,[67] especially in relation to the DGLAP equation.[34]

In particular, the analytical solution of the BK equation with running coupling can also be used to explore the core aspects of this work. The modified BK equation with running coupling differs in form from the fixed coupling case, thus requiring the determination of a new set of parameters using the available proton structure function data. According to the discussion in Ref. [55], we find that, although the form of the solution differs slightly, both fixed and running couplings can accurately describe the existing data for the cross-sections of vector meson diffraction production. We think that the difference between these two approaches does not affect the main conclusions of this work.

5. Summary. This work primarily utilizes the analytical solution of the BK equation[28] to calculate the proton structure function F_2 in the higher Q^2 region and to investigate the behavior of the structure function in the small x region. We observe that as Q^2 increases, the slope parameter λ (i.e., the rate of increase of F_2) gradually decreases and may converge at a certain value. Specifically, it approaches convergence around $\lambda \simeq 0.41 \pm 0.01$ (requiring a large Q^2 scale). On the other hand, we conduct a phenomenological analysis of the results and suggest that gluon overlap and phase space growth suppression can explain the behavior of the parameter λ.

We acknowledge that the current results are highly dependent on the approximations involved in the BK equation, particularly within the LO approximation and the fixed coupling constant approximation. While our findings currently exhibit discrepancies with experimental data, phenomenological studies of high-density gluon overlap and recombination suggest the expectation of gluon saturation characteristics in a high Q^2 region. However, this conclusion still requires validation through future high-precision electron–ion collision experiments[68–72] across a broad range of Q^2 and x.

Acknowledgements. The authors are very grateful to Dr. Rong Wang for providing suggestions about the error analysis and fruitful discussions. This work is supported by the National Key R&D Program of China (Grant Nos. 2024YFE0109800 and 2024YFE0109802), the National Natural Science Foundation of China (Grant No. 12305127), and the International Partnership Program of the Chinese Academy of Sciences (Grant No. 016GJHZ2022054FN).

References

[1] Lipatov L N 1976 *Sov. J. Nucl. Phys.* **23** 338
[2] Kuraev E A, Lipatov L N, and Fadin V S 1977 *Sov. Phys. JETP* **45** 199
[3] Balitsky I I and Lipatov L N 1978 *Sov. J. Nucl. Phys.* **28** 822
[4] Ellis J, Kowalski H, and Ross D A 2008 *Phys. Lett. B* **668** 51
[5] Kowalski H, Lipatov L N, Ross D A, and Watt G 2010 *Eur. Phys. J. C* **70** 983
[6] Kowalski H, Lipatov L N, Ross D A, and Watt G 2011 *Nucl. Phys. A* **854** 45
[7] Kowalski H, Lipatov L N, and Ross D A 2013 *Phys. Part. Nucl.* **44** 547
[8] Kowalski H, Lipatov L N, and Ross D A 2014 *Eur. Phys. J. C* **74** 2919
[9] Kowalski H, Lipatov L N, and Ross D A 2016 *Eur. Phys. J. C* **76** 23
[10] Kowalski H, Lipatov L N, Ross D A, and Schulz O 2017 *Eur. Phys. J. C* **77** 777
[11] Salam G P 1998 *JHEP* **07** 019
[12] Dokshitzer Y L 1977 *Sov. Phys. JETP* **46** 641
[13] Gribov V N and Lipatov L N 1972 *Sov. J. Nucl. Phys.* **15** 438
[14] Lipatov L N 1974 *Yad. Fiz.* **20** 181
[15] Altarelli G and Parisi G 1977 *Nucl. Phys. B* **126** 298
[16] Wilson K G 1975 *Rev. Mod. Phys.* **47** 773
[17] Mueller A H 2001 *Cargese Summer School on QCD Perspectives on Hot and Dense Matter* p. 45
[18] Staśto A M, Golec-Biernat K, and Kwieciński J 2001 *Phys. Rev. Lett.* **86** 596
[19] Munier S and Peschanski R 2003 *Phys. Rev. Lett.* **91** 232001
[20] Balitsky I 1997 *AIP Conf. Proc.* **407** 953
[21] Kovchegov Y V 1999 *Phys. Rev. D* **60** 034008
[22] Kovchegov Y V 2000 *Phys. Rev. D* **61** 074018
[23] Balitsky I 2001 *Phys. Lett. B* **518** 235
[24] Balitsky I 1996 *Nucl. Phys. B* **463** 99
[25] Jalilian-Marian J, Kovner A, Leonidov A, and Weigert H 1997 *Nucl. Phys. B* **504** 415
[26] Iancu E, Leonidov A, and McLerran L 2001 *Nucl. Phys. A* **692** 583
[27] Weigert H 2002 *Nucl. Phys. A* **703** 823
[28] Wang X, Yang Y, Kou W, Wang R, and Chen X 2021 *Phys. Rev. D* **103** 056008
[29] Bartels J and Kowalski H 2001 *Eur. Phys. J. C* **19** 693
[30] Cvetič G, Illarionov A Y, Kniehl B A and Kotikov A V 2009 *Phys. Lett. B* **679** 350
[31] Cooper-Sarkar A M, Devenish R C E, and De Roeck A 1998 *Int. J. Mod. Phys. A* **13** 3385
[32] Kotikov A V and Parente G 1999 *Nucl. Phys. B* **549** 242
[33] Kotikov A V 2007 *Phys. Part. Nucl.* **38** 1 [Erratum: 2007 *Phys. Part. Nucl.* **38** 828]
[34] Ball R D and Forte S 1994 *Phys. Lett. B* **336** 77
[35] Illarionov A Y, Kotikov A V, and Parente G 2008 *Phys. Part. Nucl.* **39** 307
[36] Mankiewicz L, Saalfeld A, and Weigl T 1997 *Phys. Lett. B* **393** 175
[37] Abramowicz H, Abt I, Adamczyk L *et al.* (H1, ZEUS) 2015 *Eur. Phys. J. C* **75** 580
[38] Luszczak A and Kowalski H 2020 *Phys. Lett. B* **802** 135199
[39] Kaidalov A B, Merino C, and Pertermann D 2001 *Eur. Phys. J. C* **20** 301
[40] Donnachie A and Landshoff P V 2003 arXiv:hep-ph/0305171

[41] Mueller A H and Patel B 1994 *Nucl. Phys. B* **425** 471
[42] Kowalski H and Teaney D 2003 *Phys. Rev. D* **68** 114005
[43] Kowalski H, Motyka L, and Watt G 2006 *Phys. Rev. D* **74** 074016
[44] de Santana Amaral J T, Gay Ducati M B, Betemps M A, and Soyez G 2007 *Phys. Rev. D* **76** 094018
[45] Barone V and Predazzi E 2002 *High-Energy Particle Diffraction* **565** (Springer-Verlag, Berlin Heidelberg)
[46] Xie Y P and Chen X 2018 *International Journal of Modern Physics A* **33** 1850034
[47] FISHER R A 1937 *Annals of Eugenics* **7** 355
[48] Wang M 1995 *Phys. Lett. A* **199** 169
[49] Wang M 1996 *Phys. Lett. A* **213** 279
[50] Zhou Y, Wang M, and Wang Y 2003 *Phys. Lett. A* **308** 31
[51] Zhou Y, Wang M, and Miao T 2004 *Phys. Lett. A* **323** 77
[52] Wang M and Li X 2014 *J. Appl. Math. Phys.* **2** 823
[53] Marquet C and Soyez G 2005 *Nucl. Phys. A* **760** 208
[54] Andreev V, Baghdasaryan A, Baghdasaryan S *et al.* (H1) 2014 *Eur. Phys. J. C* **74** 2814
[55] Wang X P, Kou W, Xie G, Xie Y P, and Chen X R 2022 *Chin. Phys. C* **46** 093101
[56] Chekanov S, Derrick M, Loizides J H *et al.* (ZEUS) 2004 *Nucl. Phys. B* **695** 3
[57] Chekanov S, Derrick M, Magill S *et al.* (ZEUS) 2007 *PMC Phys. A* **1** 6
[58] Adloff C, Andreev V, Andrieu B *et al.* (H1) 2000 *Eur. Phys. J. C* **13** 371
[59] Aktas A, Andreev V, Anthonis T *et al.* (H1) 2006 *Eur. Phys. J. C* **46** 585
[60] Aaron F D, Aldaya Martin M, Alexa C *et al.* (H1) 2010 *JHEP* **2010** 32
[61] Golec-Biernat K and Wüsthoff M 1998 *Phys. Rev. D* **59** 014017
[62] Bartels J, Golec-Biernat K, and Kowalski H 2002 *Phys. Rev. D* **66** 014001
[63] Schrempp F 2005 arXiv:hep-ph/0507160
[64] Martin A D, Roberts R G, and Stirling W J 1996 *Phys. Lett. B* **387** 419
[65] Golec-Biernat K and Wüsthoff M 1999 *Phys. Rev. D* **60** 114023
[66] Marquet C, Peschanski R, and Soyez G 2005 *Phys. Lett. B* **628** 239
[67] Mäntysaari H and Schenke B 2018 *Phys. Rev. D* **98** 034013
[68] Accardi A, Albacete J L, Anselmino M *et al.* 2016 *Eur. Phys. J. A* **52** 268
[69] Abdul Khalek R, Accardi A, Adam J *et al.* 2021 arXiv:2103.05419 [physics.ins-det]
[70] Chen X 2018 *PoS DIS* **2018** 170
[71] Chen X, Guo F K, Roberts C D, and Wang R 2020 *Few Body Syst.* **61** 43
[72] Anderle D P, Bertone V, Cao X *et al.* 2021 *Front. Phys.* **16** 64701